Supporting Information

High Mechanical Property of Laminated Electromechanical Sensors by Carbonized Nanolignocellulose/Graphene Composites

Yipeng Chen[†], *Chengmin Sheng*[†], *Baokang Dang*[†], *Temeng Qian*[†], *Chunde Jin*[†], *Qingfeng Sun*[†,*]

†School of Engineering, Zhejiang A&F University, Hangzhou, Zhejiang Province, 311300, PR China

*Corresponding author: E-mail: qfsun@zafu.edu.cn (Qingfeng Sun)

S1 Possible mechanisms leading to the variation in resistivity at low strain.

The resistance this electron feels on this part of the journey is the sum of the resistances associated with the sheets plus the resistances associated with moving from sheet to sheet: $R_{1-5}=R_{01}+R_{11}+R_{12}+R_{22}+R_{23}+R_{33}+R_{34}+R_{44}+R_{45}+R_{56}$. Here R_{11} etc represents the intra-sheet resistance, R_{12} etc represents the inter-sheet resistances and R_{01} and R_{56} represent the resistances associated with entering sheet 1 and leaving sheet 5. One should note that an intersheet resistance is always paired with an intrasheet resistance. This means that one current path through the network from one side to another via p_1 flakes has a resistance given by $R_{0-p_1} \approx \sum_{i=0}^{p_1} R_{i,i} + R_{i,i}$. If we approximate all intersheet resistances as equal and all intrasheet resistances as equal, this becomes $R_{0-n} \approx p_1(R_{i,i} + R_{i,i+1})$. While this represents one current path, there are of course many current paths operating in parallel. The total network resistance is just the sum of the contribution of all these parallel paths. If there are p_2 parallel paths and we approximate them all as equal we get: $\frac{1}{R_T} = p_2 \frac{1}{p_1(R_{i,i}+R_{i,i+1})}$. We can rewrite this as $R_T = \frac{p_1}{p_2}(R_{i,i} + R_{i,i+1})$. Given that p_1 is a measure of the number of nanosheets in a conducting path and p_2 is a measure of the number of parallel conducting paths, we would expect: $p_1 \propto L_0/l_{NS}$ and $p_2 \propto A_0$ and so $p_1/p_2 = \chi L_0/l_{NS} A_0$, where l_{NS} is the nanosheet lateral dimension and χ is a number related to the network structure. Expressed this way, χ can be roughly thought of as the cross sectional area associated with each parallel conducting path. However, we should not take the parameters p_1 and p_2 too seriously. Rather we should consider χ is a parameter which contains all the relevant information regarding the effect of network structure on electrical properties. Combing the concepts above allows us to write $R_T = \frac{\chi}{l_{NS}} \frac{L_0}{A_0} (R_{i,i} + R_{i,i+1})$, giving an expression for the network resistivity: $\rho = (R_{i,i} + R_{i,i+1})\chi/l_{NS}$

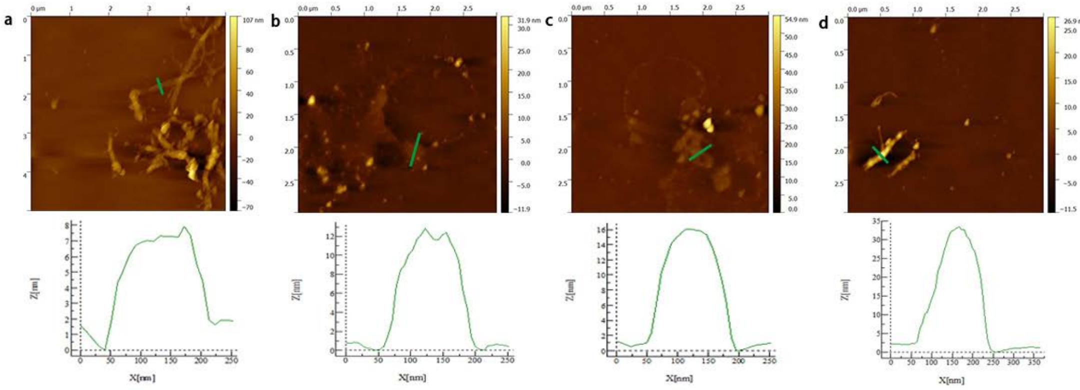

Figure S1. AFM images of (a) pure NLC, and NLC/graphene composite with (b) 0.5 wt.% (c) 1 wt.% and (d) 1.5 wt.% graphene

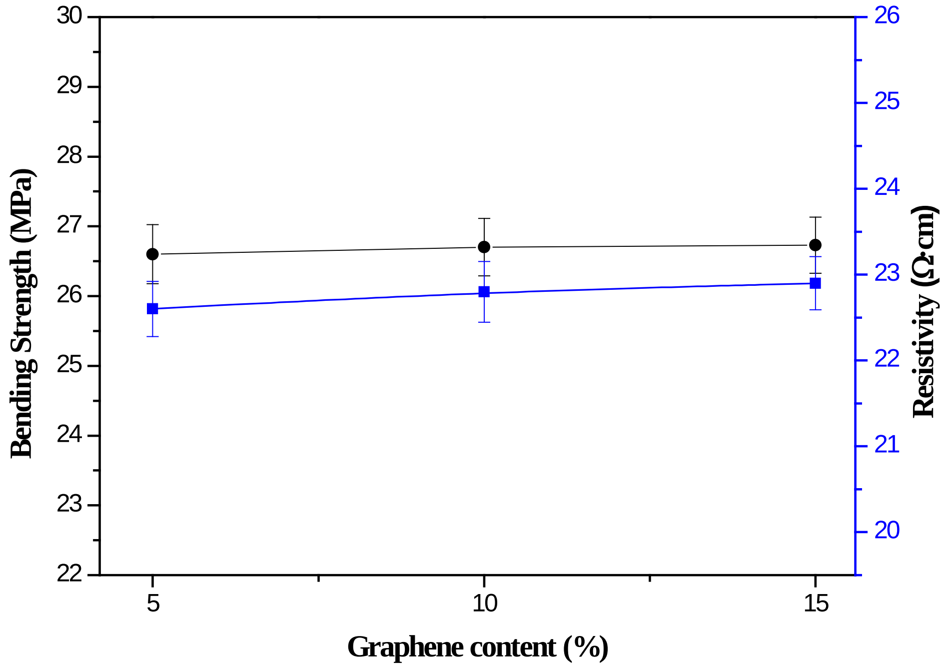

Figure S2. Bending strength and resistivity change for c-GNLC composites with different graphene loadings (from 5 to 15 wt%)

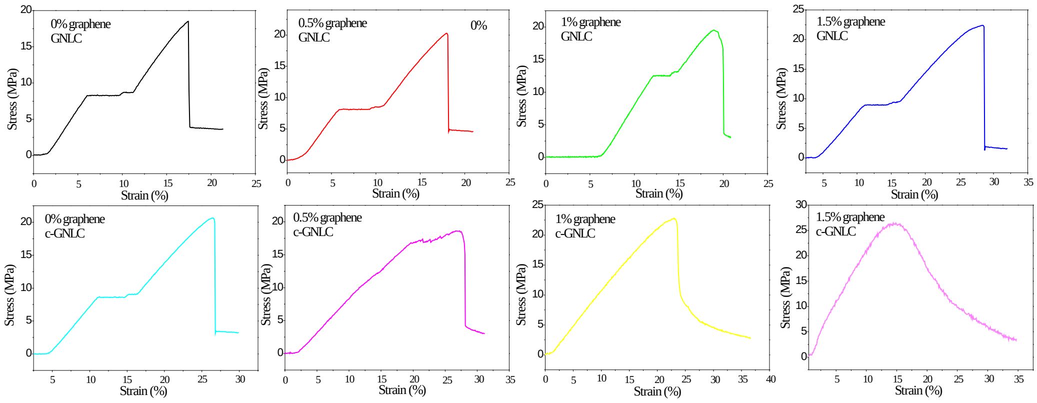

Figure S3. Stress-strain curves of c-GNLC and GNLC composites with different graphene loadings (from 0 to 1.5 wt %).

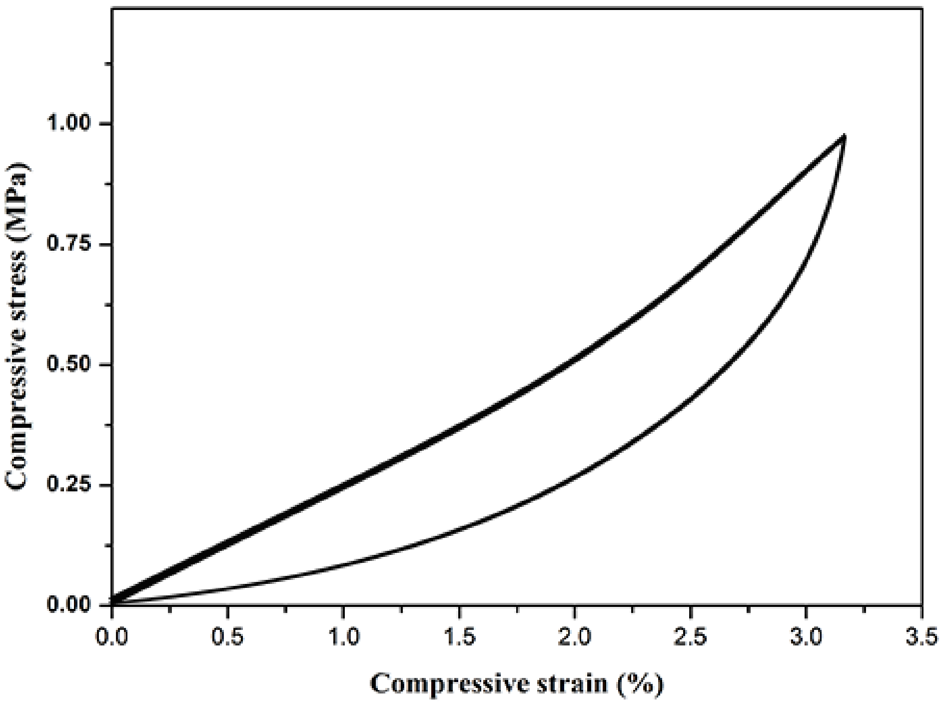

Figure S4. Stress-strain curves of the c-GNLC composites after 10 cycles

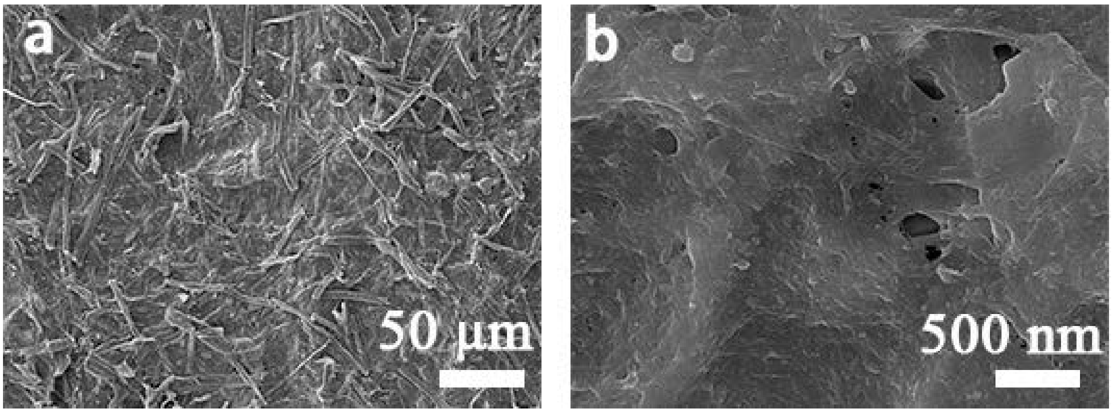

Figure S5. SEM image of (a) the surface of the c-GNLC composites, and (b) the graphene platelets on the c-NLC surface.

Table S1. Comparison of mechanical properties of our c-GNLC composite with reported lignin-based materials.

Sample	Strength (MPa)	Elastic modulus (MPa)	Ref
Carbonized/MDF[a]	17.5	4500	1
Nanoclay/Wood-based Composite	22.8	2240	2
Silicon Carbide Ceramics from Wood	18.7	6500	3
MDF[a]/melamine resin impregnated paper waste	21.8	1971	4
carbonized nanolignocellulose/graphene	25.6	2300	Our data

[a] Medium density fiberboard

Table S2 Comparison of electromechanical properties of the c-GNLC composite with reported carbon filled materials.

Sample	Repeatable Strain (%)	$\Delta R/R_0$	Sensitivity	Ref
carbon black/cement	3	0.21	0.98	5
carbon nanotube/SBS [a]	10	0.4	1.87	6
carbon nanotube/cement	3.2	0.14	0.65	7
carbon nanotube/epoxy	3	0.25	1.17	8
carbonized nanolignocellulose/graphene	3	0.24	1.14	Our data

[a] styrene-butadiene-styrene

References

1. Kercher, A. K.; Nagle, D. C. Evaluation of Carbonized Medium-Density Fiberboard for Electrical Applications. *Carbon* **2002,** 40, (8), 1321-1330.

2. Ashori, A.; Nourbakhsh, A. Effects of Nanoclay as a Reinforcement Filler on the Physical and Mechanical Properties of Wood-based Composite. *Brain Res.* **2009,** 147, (1), 159-64.

3. Greil, P.; Lifka, T.; Kaindl, A. Biomorphic Cellular Silicon Carbide Ceramics from Wood: II. Mechanical Properties. *J. Eur. Ceram. Soc.* **1998,** 18, (14), 1975-1983.

4. Ayrilmis. Enhancement of Dimensional Stability and Mechanical Properties of Light MDF By Adding Melamine Resin Impregnated Paper Waste. *Int. J. Adhes. Adhes.* **2012,** 33, (3), 45-49.

5. Xiao, H.; Li, H.; Ou, J. Modeling of Piezoresistivity of Carbon Black Filled Cement-Based

Composites under Multi-Axial Strain. *Sensors Actuat. A Phys.* **2010,** 160, (1–2), 87-93.

6. Costa, P.; Ribeiro, S.; Lanceros-Mendez, S. Mechanical vs. Electrical Hysteresis of Carbon Nanotube/Styrene-Butadiene-Styrene Composites and Their Influence In The Electromechanical Response. *Compos. Sci. Technol.* **2015,** 109, 1-5.

7. Li, G. Y.; Wang, P. M.; Zhao, X. Pressure-Sensitive Properties and Microstructure of Carbon Nanotube Reinforced Cement Composites. *Cement Concrete Comp.* **2007,** 29, (5), 377-382.

8. Gui, X.; Li, H.; Zhang, L.; Jia, Y.; Liu, L.; Li, Z.; Wei, J.; Wang, K.; Zhu, H.; Tang, Z. A Facile Route to Isotropic Conductive Nanocomposites by Direct Polymer Infiltration of Carbon Nanotube Sponges. *Acs Nano* **2011,** 5, (6), 4276-83.